European Journal of Neurology

european journal of neurology
the official journal of the european academy of neurology

ORIGINAL ARTICLE OPEN ACCESS

Progressive Thalamo-Cortical Disconnection in Amyotrophic Lateral Sclerosis Genotypes: Structural Degeneration and Network Dysfunction of Thalamus-Relayed Circuits

Marlene Tahedl[1] | Jana Kleinerova[1] | Mark A. Doherty[2] | Jennifer C. Hengeveld[2] | Russell L. McLaughlin[2] | Orla Hardiman[1] | Ee Ling Tan[1] | Peter Bede[1,3]

[1]Computational Neuroimaging Group (CNG), School of Medicine, Trinity College Dublin, Dublin, Ireland | [2]Complex Trait Genomics Laboratory, Smurfit Institute of Genetics, Trinity College Dublin, Dublin, Ireland | [3]Department of Neurology, St James's Hospital, Dublin, Ireland

Correspondence: Peter Bede (bedep@tcd.ie)

Received: 2 February 2025 | **Revised:** 12 March 2025 | **Accepted:** 27 March 2025

Funding: This study was supported by the Health Research Board (HRB EIA-2017-019 & JPND-Cofund-2-2019-1), the EU Joint Programme—Neurodegenerative Disease Research (JPND), and Science Foundation Ireland (SFI SP20/SP/8953). Genetic aspects of the study were supported by the MND Association (898-792) and Science Foundation Ireland (17/CDA/4737).

Keywords: amyotrophic lateral sclerosis | magnetic resonance imaging | motor neuron disease | neuroimaging

ABSTRACT

Background: The thalamus is a key subcortical hub of numerous corticobasal and corticocortical circuits mediating a wealth of cognitive, behavioural, sensory and motor processes. While thalamic pathology is increasingly recognised in amyotrophic lateral sclerosis, its degeneration is often assessed in isolation instead of adopting a network-wise perspective and assessing the integrity of its rich cortical projections.

Methods: A prospective imaging study was conducted in a cohort of genetically stratified patients to assess the structural and functional integrity of thalamo-cortical circuits and volumetric alterations longitudinally.

Results: The white matter integrity of thalamic projections to the anterior cingulate cortex, cerebellum, dorsolateral prefrontal cortex (DLPFC), Heschl's gyrus, medial frontal gyrus (MFG), orbitofrontal cortex, parietal cortex, postcentral gyrus and precentral gyrus (PreCG) is affected at baseline in ALS, which is more marked in *C9orf72* hexanucleotide repeat carriers. Precentral gyrus and cerebellar grey matter volumes are also reduced, particularly in *C9orf72*. *Longitudinal* analyses capture progressive disconnection between the thalamus and frontal regions (DLPFC and MFG) in both *C9orf72* positive and sporadic patients and progressive thalamo-PreCG disconnection in the sporadic *C9orf72* negative cohort. Functional connectivity analyses revealed

Abbreviations: ACC, anterior cingulate cortex; ALS, amyotrophic lateral sclerosis; ALSFRS-r, ALS functional rating scale; ANOVA, analysis of variance; ATX, patients carrying an intermediate-length CAG repeat expansion in ATXN2; BOLD, blood-oxygen-level-dependent (BOLD) signal; C9NEG, sporadic ALS patients who tested negative for a panel of ALS-associated genetic variants as well as GGGGCC hexanucleotide repeat expansion in *C9orf72*; C9POS, GGGGCC hexanucleotide repeat expansion carriers in *C9orf72*; CSD, constrained spherical deconvolution; CTh, cortical thickness; DKI, diffusion kurtosis imaging; DLPFC, dorsolateral prefrontal cortex; dMRI, diffusion-weighted MRI; EPI, echo-planar imaging; FA, fractional anisotropy; FC, functional connectivity; fMRI, functional MRI; fODF, fibre orientation distribution function; FOV, field of view; FSL, FMRIB′′s Software Library; GM, greygray matter; HARDI, high-angular resolution diffusion imaging; HC, healthy control; IQR, interquartile range; IR-SPGR, inversion recovery prepared spoiled gradient recalled echo; MFG, medial frontal gyrus; ML, Machine learning; MND, Motor neuron disease; MNI152, Montreal Neurological Institute 152 standard space; MRI, magnetic resonance imaging; NODDI, neurite orientation dispersion and density imaging; OFC, orbitofrontal cortex; PostCG, postcentral gyrus; PreCG, precentral gyrus; RD, Radial diffusivity; ROI, region of interest; rs-fMRI, resting-state functional MRI; SC, structural connectivity; SD, standard deviation; SE-EPI, spin echo planar imaging; T, Tesla; T1w, T1-weighted imaging; TE, echo time; TI, inversion time; TR, repetition time; UMN, upper motor neuron; V1, primary visual cortex.; VR, voxel resolution; WM, white matter.

increasing thalamo-cerebellar connectivity in sporadic ALS and increasing thalamo-DLPFC connectivity in intermediate-length CAG repeat expansion carriers in *ATXN2* over time.

Discussion: Our data provide evidence of extensive thalamo-cortical connectivity alterations in ALS. Corticobasal circuits mediating extrapyramidal, somatosensory, cognitive and behavioural functions are increasingly affected as the disease progresses. The degeneration of thalamic projections support the conceptualisation of ALS as a 'network disease' and the notion of 'what wires together degenerates together'.

1 | Introduction

There is considerable neuroimaging and post-mortem evidence of significant thalamic disease burden in ALS. Early studies of ALS tend to evaluate the thalamus as a single structure, evaluating overall volumes and surface deformations [1], whilst more recent ALS studies have segmented the thalamus into distinct nuclei, functional subregions or according to cortical connectivity patterns [2, 3]. The involvement of the thalamus has also been demonstrated in ALS by robust functional and metabolic imaging studies [4–6]. There is ample post-mortem evidence of thalamic pathology in ALS [7] and thalamic involvement is regarded to be a stage-defining feature of pTDP-43 propagation [8]. Hexanucleotide repeat expansion carrier status in *C9orf72* is thought to be associated with thalamic vulnerability [4, 9] with a predilection for specific subregions [10].

The physiological role of the thalamus is relaying thermoceptive, nociceptive, proprioceptive and vibrioceptive information through the ventral posterolateral nuclei; auditory inputs via the medial geniculate nuclei; gustatory information via the ventral medial nuclei; and visual afferents through the lateral geniculate nuclei are widely known [11]. However, the non-sensory functions of the thalamus are often overlooked. Limbic functions are relayed through anterior, dorsal and pulvinar nuclei [11, 12]; language processes are conveyed by ventral nuclei [11] and the intralaminar and reticular nuclei play a physiological role in arousal and alertness [11]. Associative processes are relayed through midline nuclei [11, 12] which contribute to the reconciliation of somatosensory and visuospatial information [11]. The anterior nuclei are important hubs of the Papez circuit [13] which is known to be affected in ALS [14–16]. The physiological role of thalamus-mediated cognitive and behavioural functions has an ever-increasing literature and is now supported by complex human neuroimaging studies [12, 13, 17, 18].

The clinical, genetic and neuroimaging overlap between ALS and FTD is well recognised [3, 19] with shared imaging patterns, genetic variants and comorbid presentations. Thalamic pathology and thalamo-cortical connectivity alterations are well recognised in FTD [10] and there is a wealth of neuroimaging literature highlighting thalamic involvement in FTD [20] and its specific clinical manifestations [21]. The FTD imaging literature demonstrates the important neuropsychological manifestations of thalamic pathology, highlighting how focal thalamic changes may manifest in specific cognitive and behavioural deficits [21]. The physiological role of specific cortico-thalamic networks in mediating specific executive, language and behavioural functions is well described [18, 22]. Both the ALS and FTD literature suggest that subcortical changes do not occur in isolation, but mirror cortical atrophy patterns, and interconnected cortical and subcortical foci exhibit concomitant degeneration [2, 21, 23, 24]. This is in line with clinical observations [23, 24] supporting the conceptualisation of ALS-FTD as a network disease or circuitry dysfunction, rather than the manifestation of focal cortical disease. The demonstration of focal subcortical disease and associated cortical disease seems to be consistent with 'prion-like' trans-synaptic propagation hypotheses [25]. Accordingly, insights from the ALS-FTD spectrum not only confirm phenotype-defining clinical manifestations of thalamic disease burden but also indicate a central role in disease propagation. With the recognition of pre-manifest or pre-symptomatic processes, there is increasing evidence of thalamic involvement in both ALS and FTD [26–31]. Despite the consensus of thalamic volume reductions in ALS-FTD, studies evaluating progressive thalamic changes over time are somewhat inconsistent [1, 32].

In light of the existing literature, we aim to look beyond focal thalamic pathology and examine the connectivity patterns of the structure to specific cortical and cerebellar regions. Our objective is the comprehensive characterisation of cortico-thalamic connectivity using both structural and functional approaches and to explore if genotype specific patterns exist. Additionally, we sought to establish if progressive longitudinal changes occur in the symptomatic phase of the disease.

2 | Methods

2.1 | Participants

A total of 263 participants, 150 patients with ALS and 113 healthy controls (HC) were enrolled in this study. All participants gave informed consent in accordance with the Ethics Approval of this research study (Beaumont Hospital, Dublin, Ireland). ALS patients were stratified by their genetic status: patients carrying GGGGCC hexanucleotide repeat expansions in *C9orf72* ('C9POS' $N=15$), sporadic patients testing negative for a panel of ALS-associated genetic variants as well as *C9orf72* repeat expansions ("C9NEG", $N=130$) and patients carrying an intermediate-length CAG repeat expansion in *ATXN2* ("ATX", $N=5$). Methods for genetic screening are summarised in Data S1. Longitudinal neuroimaging with four MRI sessions was organised with an inter-scan interval of 4 months (111–135 days). Core demographic and clinical data were systematically recorded, including age, sex, symptom duration, time of diagnosis, handedness, education, site of disease onset, ALS functional rating scale (ALSFRS-r) (Table S1). Exclusion criteria for HC encompassed neurological or psychiatric disease and a family history of ALS. Participating

ALS patients had "definite ALS" according to the revised El Escorial criteria.

2.2 | Neuroimaging

Scanner parameters and the neuroimaging protocol have been previously described [33], but are also summarised in Data S2. Eleven physiologically relevant [18, 22, 34] cortico-thalamic networks were selected and cortical regions of interest (ROIs) defined accordingly: (1) The anterior cingulate cortex (ACC) due to its role in the 'anterior cingulate circuit' mediating executive function; (2) cerebellar cortex, due to its involvement in ALS [35, 36]; (3) dorsolateral prefrontal cortex (DLPFC) due to its role in the 'dorsolateral prefrontal circuit' conveying executive function; (4) Heschl's gyrus given its contribution to auditory function mediated via the medial geniculate nucleus; (5) mammillary bodies as they form part of the 'Papez circuit'; (6) medial frontal gyrus (MFG) as it is implicated in apathy; (7) orbitofrontal cortex (OFC) as it's part of to 'orbitofrontal circuit'; (8) parietal cortex given their diverse role in various cognitive functions [37]; (9) postcentral gyrus (PostCG) due to it central role in sensory processing; (10) precentral gyrus (PreCG) as a primary motor region; (11) primary visual cortex (V1) given its association with the lateral geniculate nucleus. Each cortical region was defined in "subject space" using atlas parcellation schemes summarised in Table S2.

2.3 | Volumetry

To assess grey matter (GM) alterations in ALS genotypes, we calculated thalamic and cortical ROI volumes. T1w data were pre-processed using the Computational Anatomy Toolbox (CAT12), which is an extension to the SPM12 toolbox (Wellcome Department of Cognitive Neurology). Preprocessing steps include denoising, affine registration to the bias-corrected image to improve downstream Local Adaptive Segmentation (LAS). LAS is an intensity transformation step applied to all tissue classes to enhance the accuracy of downstream Adaptive Maximum A Posterior (AMAP) segmentation, which models local variations of the parameters as slowly varying spatial functions to correct for both intensity inhomogeneities as well as local intensity variations. Subsequently, partial volume segmentation, skull-stripping and spatial normalisation were performed. Spatial normalisation relies on the integration of the Dartel and Geodesic Shooting normalisation, which is based on existing templates in Montreal Neurological Institute (MNI) space. The CAT12 pipeline enables the registration of commonly used atlases in subject space and the estimation of ROI GM volumes and total intracranial volume (TIV). In this study, we used labels from the Automated Anatomical Labelling Atlas version 3 (AAL3) for cortical ROIs; the Spatially Unbiased Infratentorial Template (SUIT) for the cerebellum; the Computational Brain Anatomy Laboratory atlas (CoBrA) for the mammillary bodies. GM volume estimates for the ROIs were calculated in CAT12, extracted and averaged across hemispheres. The thalamus was defined using the 'recon-all' pipeline of FreeSurfer, which includes thalamic segmentation and volume estimation in subject space (Table S2).

2.4 | Structural Connectivity

Microstructural white matter (WM) integrity of eleven different thalamic projections was estimated using tractography. dMRI data were pre-processed using the standard MRtrix3 pipeline, which includes noise removal, Gibb's Ringing artefact removal, motion, eddy current and bias field corrections. Fibre orientation distribution (fODF) was then estimated in each voxel using constrained spherical deconvolution (CSD) and further normalised. The main advantage of CSD as compared to commonly-used tensor-based models is its enhanced accuracy in resolving multiple fibre orientations in voxels containing crossing fibres even at low *b*-values. The tracts-of-interest were defined in each individual subject by first generating 5000 streamlines between the thalamus and the eleven target ROIs bilaterally. Streamlines were generated using probabilistic tractography. Outputs are illustrated in Figure 1. Track data were mapped onto a high-resolution image in subject space using Track Density Imaging (TDI). The resulting images were binarised to produce maps, which we used to extract average fractional anisotropy (FA) and average radial diffusivity (RD) per tract.

2.5 | Functional Connectivity

To evaluate functional connectivity (FC) changes, we calculated correlations of the BOLD signal between the thalamus and the eleven target ROIs. rs-fMRI data were pre-processed using the standardised *feat* pipeline from the FMRIB Software Library (FSL) which includes brain extraction, intensity normalisation, and slice-time correction. We corrected for head-motion artefacts using FSL's ICA-based Automatic Removal of Motion Artefacts (ICA-AROMA) and complemented data cleaning with regression of confounding effects of WM and cerebrospinal fluid (CSF). The cleaned data were transformed into MNI152 2 mm standard space by combining an initial linear co-registration of the native functional to the native high-resolution structural image using 6° of freedom (DOFs), followed by non-linearly warping into standard space using 12 DOFs. We calculated FC between the thalamus and the eleven target ROIs within Matlab R2022b (The Mathworks, Natick, USA), making use of the CoSMoMVPA as Fisher z-transformed Pearson correlation coefficient between the mean BOLD time course of each pair of ROIs.

2.6 | Statistical Modelling

Statistical inferences were computed within RStudio, version 2022.12.0 + 353 (based on R version 4.2.2). Differences in means of age and education between all ALS patients (aggregating across genotypes) and HC were investigated using Welch two-sample *t*-tests, whereas differences in sex and handedness frequencies were compared using Chi-square testing. To test for cross-sectional differences in neuroimaging metrics between patient genotypes and HC, a one-way analysis of variance (ANOVA) was implemented, correcting for confounding effects of age, sex, handedness, years of education and symptom duration (the latter only for ALS patients). In volumetric analyses, we additionally corrected for

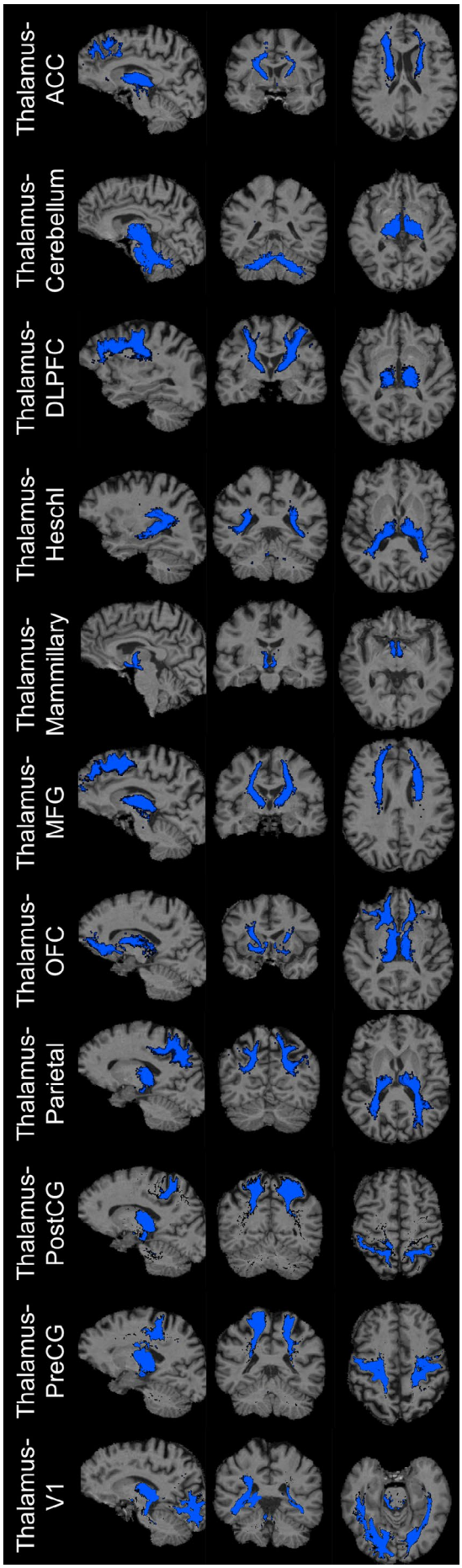

FIGURE 1 | Thalamo-cortical tractography. Representative tractography outputs between the thalamus and 11 cortical regions of interest. Sagittal, coronal and axial views are presented from left to right for each cortical projection. ACC, anterior cingulate cortex; DLPFC, dorsolateral prefrontal cortex; Heschl, Heschl's gyrus; Mammillary, mammillary bodies; MFG, medial frontal gyrus; OFC, orbitofrontal cortex; Parietal, parietal cortex; PostCG, postcentral gyrus; PreCG, precentral gyrus; V1, primary visual cortex.

the total intracranial volume (TIV). For each comparison, we evaluated the main effect of *Group* (i.e., ALS genotype/HC), and where significant, we further explored pairwise differences in groups using post hoc testing with Tukey's Honest Significant Difference (Tukey HSD). We report as adjusted *p*-values (p_{adj}), accounting for all possible pairs of comparisons. To test for longitudinal differences between ALS genotypes and HC, a linear mixed effects model was implemented (using R's *nmle* package). In that model, we defined *Time* (i.e., session) as a random effect and the subject identifier as fixed effects. We corrected for confounding effects of age, sex, handedness, years of education and symptom duration (latter only for ALS patients). In volumetric analyses, we additionally corrected for TIV. For each comparison, we evaluated the interaction effect '*Time* x *ALS Genotype*' versus '*Time* × *HC*' (i.e., we used HC as reference group in the model). Analogous to the cross-sectional comparisons, we used *p*-values at ≤0.05 as indicative of significant differences.

3 | Results

3.1 | Subjects

A total of 150 patients with ALS (15 C9POS, 130 C9NEG, 5 ATX) and 113 HC were included. The majority of patients and some controls had longitudinal data with up to three follow-up scans. Multimodal MRI with T1w, dMRI and rs-fMRI data were available for most but not all participants (Table S1). Patients and controls were matched for age ($t(250.39) = 0.027$, p =. 979) and handedness ($X^2(1, N = 150) = 0.264$, $p = 0.608$). The ALS cohort had fewer years of education ($t(239.77) = -2.92$, $p = 0.004$) and relatively more males compared to HC ($X^2(1, N = 150) = 9.06$, $p = 0.003$).

3.2 | Cross-Sectional Connectivity

Figure 2 summarises the main tractographic findings and Table 1 provides the statistical details. ANOVAs captured SC differences between the four study groups for most projections, including the ones to the ACC, cerebellum, DLPFC, Heschl's gyrus, MFG, OFC, parietal cortex, PostCG, and PreCG. No integrity differences were identified in mammillary and visual cortex projections. Post hoc testing indicated that group differences were mostly driven by *C9orf72* positive patients (higher RD, lower FA) particularly when compared to controls, but in some tracts also in comparison to C9NEG (Table 1). No differences were detected for the ATX genotype, which may be due to insufficient power ($N = 5$). Interestingly, RD was more sensitive

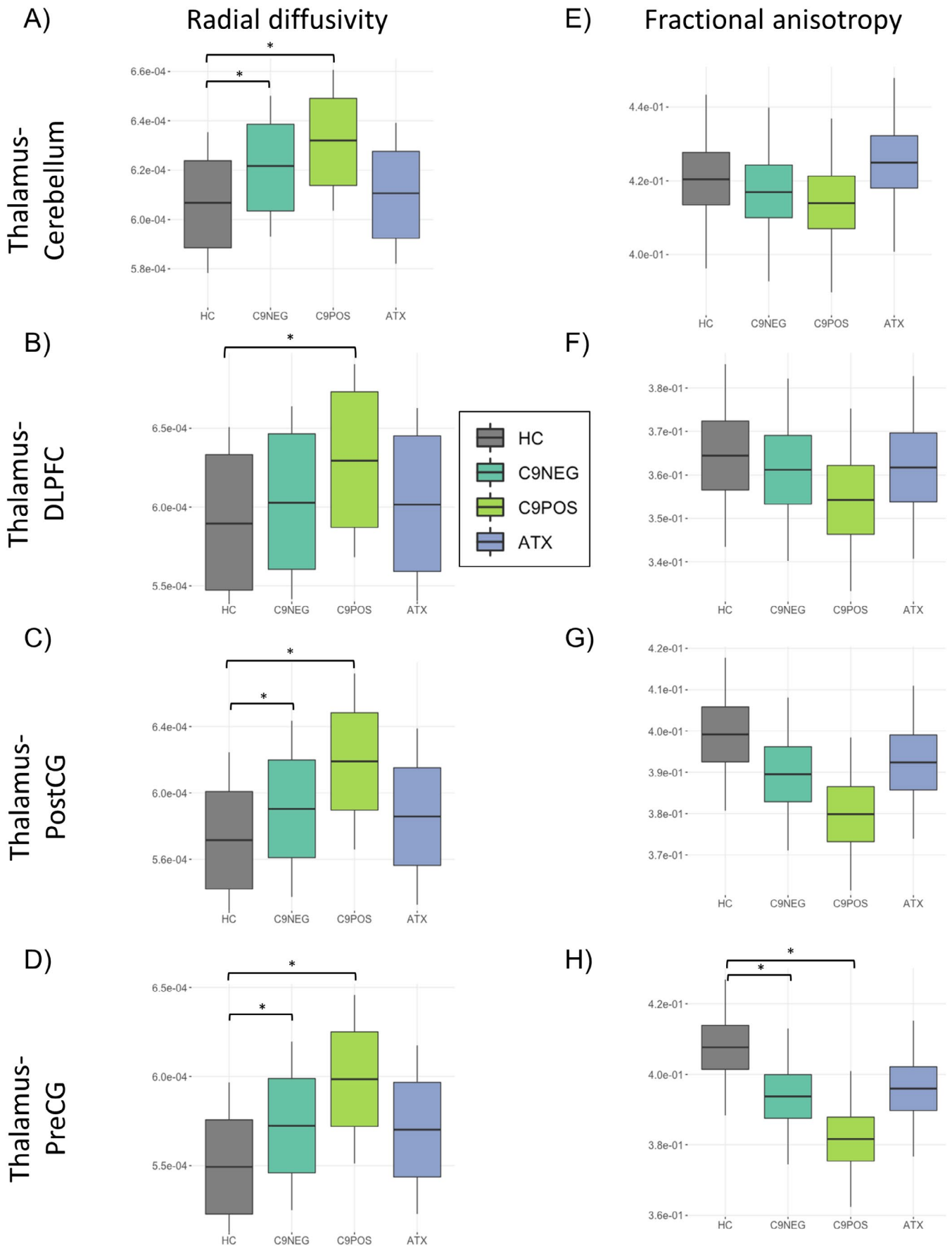

FIGURE 2 | Legend on next page.

FIGURE 2 | Cross-sectional structural connectivity (SC) profiles. Radial diffusivity (RD) distributions are shown on the left (A-D), fractional anisotropy (FA) profiles on the right (E-H). * indicates adjusted $p \leq 0.05$ in post hoc pairwise comparisons using Tukey's HSD testing. ATX, Patients with ALS carrying an intermediate length CAG repeat expansion in *ATXN2*, C9NEG = Sporadic patients with ALS testing negative for ALS associated genetic variants as well as *C9orf72* hexanucleotide repeat expansions; C9POS, Patients with ALS carrying GGGGCC hexanucleotide repeat expansions in C9orf72; DLPFC, dorsolateral prefrontal cortex; HC, healthy controls; PostCG, postcentral gyrus; PreCG, precentral gyrus.

in detecting tract integrity changes compared to FA, which is illustrated in Figure 2. For projections between the thalamus and PreCG, both metrics indicated disconnection in C9POS and C9NEG genotypes. We failed to identify group differences in functional connectivity between the study groups (Figure 3A–C and Table 1).

3.3 | Cross-Sectional Volumetry

Figure 3D,E summarises the main volumetric findings. Global atrophy was detected in the C9POS group as indicated by lower TIV compared to all other ALS genotypes as well as HC. Focal atrophy was only detected in some target ROIs, including the PreCG and the cerebellar cortex, but not the thalamus. The C9POS group was more affected in these regions than the other study groups. Comprehensive statistical details are provided in Table 1.

3.4 | Longitudinal Structural Connectivity

Few longitudinal changes were identified SC between the study groups (Figure 4). Progressive disconnection was identified between the thalamus and frontal regions (DLPFC and MFG) in both C9POS and C9NEG compared to controls. Moreover, progressive thalamo-PreCG disconnection was observed for C9NEG, as indicated by both increasing RD and decreasing FA. Similar to the cross-sectional findings of the study, we found that RD was superior in detecting progressive changes compared to FA. Comprehensive statistical details are provided in Table 2.

3.5 | Longitudinal Functional Connectivity

Linear mixed effects models were used to evaluate longitudinal FC changes. In brief, longitudinal comparisons of FC trajectories yielded few significant differences (Figure 4); increasing thalamo-cerebellar FC was detected in C9NEG ($t(187) = 2.08$, $p = 0.039$) and increasing thalamo-DLPFC FC was identified in ATX ($t(194) = 2.41$, $p = 0.017$) compared to controls over time.

3.6 | Longitudinal Volumetry

Decreasing cerebellar cortex volume was detected in C9NEG patients ($t(200) = 2.08$, $p = 0.039$) over time compared to controls. In C9POS, decreasing OFC ($t(200) = -3.00$, $p = 0.003$, Figure 4) and PreCG volume was noted compared to controls ($t(200) = -2.17$, $p = 0.031$, Figure 4). There was a tendency for more rapid TIV decline in ATX versus HC over time ($t(200) = -1.92$, $p = 0.056$). No progressive thalamic atrophy was identified in the study groups. Further statistical details are presented in Table 2.

4 | Discussion

Our data demonstrate thalamo-cortical disconnection in ALS, which is particularly marked in GGGGCC hexanucleotide repeat carriers in *C9orf72*. While there is a plethora of reports of precentral gyrus, frontotemporal and more recently of cerebellar grey matter degeneration in ALS, we demonstrate that white matter bundles connecting these regions to the thalamus show concomitant degeneration. We demonstrate that white matter projections from the thalamus to the anterior cingulate cortex, cerebellum, dorsolateral prefrontal cortex, Heschl's gyrus, medial frontal gyrus, orbitofrontal cortex, parietal cortex, postcentral gyrus and precentral gyrus are all affected. This is in line with the rich clinical literature of cognitive dysfunction, behavioural impairment, deficits in social cognition, apathy, extrapyramidal manifestations and somatosensory alterations in ALS [38–41].

In accordance with previous reports, precentral gyrus and cerebellar grey matter volumes are significantly reduced in ALS, particularly in *C9orf72*. *Longitudinal* white matter analyses capture progressive disconnection between the thalamus and frontal regions (DLPFC and MFG) in both *C9orf72* positive and sporadic patients and progressive thalamo-PreCG disconnection in the sporadic *C9orf72* negative cohort. Progressive thalamo-frontal disconnection, irrespective of *C9orf72* status, is likely to contribute to the multitude of progressive neuropsychological deficits observed in ALS. The dorsolateral prefrontal circuit is a key mediator of executive function [18, 22] and medial frontal gyrus (MFG) pathology has been consistently implicated in apathy [18, 22].

Fronto-thalamic circuits have also been associated with language function [42], decision making [43], and cognitive reasoning [44]. Progressive thalamo-primary motor cortex (PreCG) disconnection in the large sporadic cohort is not surprising either, as progressive motor network degeneration is one of the hallmarks of ALS [33]. We identified increasing thalamo-cerebellar functional connectivity in C9NEG and increasing thalamo-DLPFC FC in ATX. While motor reserve, adaptive and compensatory processes have been previously suggested in ALS [45, 46], there is no post mortem evidence for hypertrophic changes, and we found no supportive evidence from our diffusivity data.

Similar to previous white matter connectivity analyses in motor neuron diseases [33, 47], RD seems to be the most sensitive marker of white matter degeneration, both in detecting baseline WM pathology as well as capturing progressive changes over short follow-up intervals. It outperforms both FA, but particularly FC, which barely captures longitudinal changes. There is a striking paucity of longitudinal imaging studies in ALS, despite the fact that only such studies

TABLE 1 | Cross-sectional comparisons of neuroimaging metrics between ALS genotypes vs. healthy controls.

	One-way ANOVAs (omnibus tests, main effect: "Group")			
	F*(DOF), *p	***p* Significant pairwise contrasts (post hoc)**	***F*(DOF), *p***	***p* Significant pairwise contrasts (post hoc)**
Connectivity				
Connectivity: *Thalamus-Anterior cingulate cortex*			*Connectivity*: *Thalamus-Cerebellar cortex*	
SC:FA	$F(3,246) = 1.35$, $p = 0.258$	n.a.	$F(3,246) = 1.32$, $p = 0.270$	n.a.
SC:RD	$F(3,246) = 4.45$, $p = 0.005$	- C9NEG—HC [$p_{adj} = 0.002$]	$F(3,246) = 6.94$, $p < 0.001$*	- C9NEG—HC [$p_{adj} < 0.001$]—C9POS—HC [$p_{adj} = 0.027$]
FC	$F(3,235) = 0.210$, $p = 0.890$	n.a.	$F(3,235) = 0.244$, $p = 0.866$	n.a.
Connectivity: *Thalamus-Dorsolateral prefrontal cortex*			*Connectivity*: *Thalamus-Heschl's gyrus*	
SC:FA	$F(3,246) = 0.713$, $p = 0.545$	n.a.	$F(3,246) = 1.09$, $p = 0.356$	n.a.
SC:RD	$F(3,246) = 4.65$, $p = 0.003$*	- C9POS—HC [$p_{adj} = 0.017$]	$F(3,246) = 1.09$, $p = 0.005$*	- C9POS—HC [$p_{adj} = 0.009$]
FC	$F(3,235) = 0.447$, $p = 0.719$	n.a.	$F(3,235) = 1.40$, $p = 0.244$	n.a.
Connectivity: *Thalamus-Mammillary bodies*			*Connectivity*: *Thalamus-Medial frontal gyrus*	
SC:FA	$F(3,246) = 1.90$, $p = 0.131$	n.a.	$F(3,246) = 0.983$, $p = 0.401$	n.a.
SC:RD	$F(3,246) = 1.52$, $p = 0.210$	n.a.	$F(3,246) = 4.11$, $p = 0.007$	- C9POS—HC [$p_{adj} = 0.038$]
FC	$F(3,235) = 1.93$, $p = 0.126$	n.a.	$F(3,235) = 0.183$, $p = 0.908$	n.a.
Connectivity: *Thalamus-Orbitofrontal cortex*			*Connectivity*: *Thalamus-Parietal cortex* (*no postcentral gyrus*)	
SC:FA	$F(3,246) = 3.14$, $p = 0.026$	- C9POS—HC [$p_{adj} = 0.044$]	$F(3,246) = 1.15$, $p = 0.331$	n.a.
SC:RD	$F(3,246) = 2.62$, $p = 0.051$	n.a.	$F(3,246) = 3.20$, $p = 0.024$	n.a.

(Continues)

TABLE 1 | (Continued)

	One-way ANOVAs (omnibus tests, main effect: "Group")			
	F*(DOF), *p	***p*** **Significant pairwise contrasts (post hoc)**	***F*(DOF), *p***	***p*** **Significant pairwise contrasts (post hoc)**
FC	$F(3,235)=0.194$, $p=0.900$	n.a.	$F(3,235)=0.146$, $p=0.932$	n.a.
Connectivity: *Thalamus-Postcentral gyrus*			*Connectivity*: *Thalamus-Precentral gyrus*	
SC:FA	$F(3,246)=2.77$, $p=0.043$*	n.a.	$F(3,246)=6.18$, $p<0.001$*	- C9NEG—HC [$p_{adj}=0.008$] - C9POS—HC [$p_{adj}=0.004$]
SC:RD	$F(3,246)=7.16$, $p<0.001$*	- C9NEG—HC [$p_{adj}=0.029$] - C9POS—HC [$p_{adj}=0.001$]	$F(3,246)=10.72$, $p<0.001$*	- C9NEG—HC [$p_{adj}<0.001$] - C9POS—HC [$p_{adj}<0.001$]
FC	$F(3,235)=1.15$, $p=0.330$	n.a.	$F(3,235)=0.071$, $p=0.546$	n.a.
Connectivity: *Thalamus-Primary visual cortex*				
SC:FA	$F(3,246)=0.363$, $p=0.800$	n.a.		
SC:RD	$F(3,246)=1.53$, $p=0.207$	n.a.		
FC	$F(3,235)=0.304$, $p=0.823$	n.a.		
Volumetry				
Volume: *Total grey matter*			*Volume*: *Thalamus*	
	$F(3,250)=13.07$, $p<0.001$*	- C9POS—HC [$p_{adj}<0.001$] - C9POS—C9NEG [$p_{adj}<0.001$] - ATX—C9POS [$p_{adj}=0.002$]	$F(3,250)=1.18$, $p=0.319$	n.a.

(Continues)

TABLE 1 | (Continued)

	One-way ANOVAs (omnibus tests, main effect: "Group")			
	F*(DOF), *p	***p* Significant pairwise contrasts (post hoc)**	***F*(DOF), *p***	***p* Significant pairwise contrasts (post hoc)**
Volume: *ACC*			*Volume*: *Cerebellar cortex*	
	$F(3,250) = 0.894$, $p = 0.445$	n.a.	$F(3,250) = 4.81$, $p = 0.003$*	- C9POS—HC [$p_{adj} = 0.051$] - C9POS—C9NEG [$p_{adj} = 0.047$] - ATX—C9POS [$p_{adj} = 0.016$]
Volume: *Dorsolateral prefrontal cortex*			*Volume*: *Heschl's gyrus*	
	$F(3,250) = 1.24$, $p = 0.295$	n.a.	$F(3,250) = 1.84$, $p = 0.141$	n.a.
Volume: *Mammillary bodies*			*Volume*: *Medial frontal gyrus*	
	$F(3,250) = 0.937$, $p = 0.423$	n.a.	$F(3,250) = 0.637$, $p = 0.591$	n.a.
Volume: *Orbitofrontal cortex*			*Volume*: *Parietal cortex* (*no postcentral gyrus*)	
	$F(3,250) = 0.281$, $p = 0.839$	n.a.	$F(3,250) = 3.29$, $p = 0.021$*	n.a.
Volume: *Postcentral gyrus*			*Volume*: *Precentral gyrus*	
	$F(3,250) = 1.78$, $p = 0.152$	n.a.	$F(3,250) = 13.33$, $p < 0.001$*	- C9POS—HC [$p_{adj} < 0.001$]—C9POS—C9NEG [$p_{adj} < 0.001$]—ATX—C9POS [$p_{adj} = 0.003$]
Volume: *Primary visual cortex*				
	$F(3,250) = 0.688$, $p = 0.560$	n.a.		

Abbreviations: adj, adjusted; ALS, amyotrophic lateral sclerosis; ANOVA, analysis of variance; ATX, Patients with ALS carrying an intermediate length CAG repeat expansion in *ATXN2*; C9NEG, Sporadic patients with ALS testing negative for ALS-associated genetic variants as well as *C9orf72* hexanucleotide repeat expansions; C9POS, Patients with ALS carrying GGGGCC hexanucleotide repeat expansions in *C9orf72*; dMRI, diffusion-weighted magnetic resonance imaging; DOF, degrees of freedom; FA, fractional anisotropy; FC, functional connectivity; HC, healthy control; HSD, honest significant difference; n.a, not applicable (here: ANOVA omnibus test was not significant and therefore post hoc testing was not justified); RD, radial diffusivity; rs-fMRI, resting-state functional magnetic resonance imaging; SC, structural connectivity; T1w, T1-weighted.
*Significant at an alpha-level of $p \leq 0.05$.

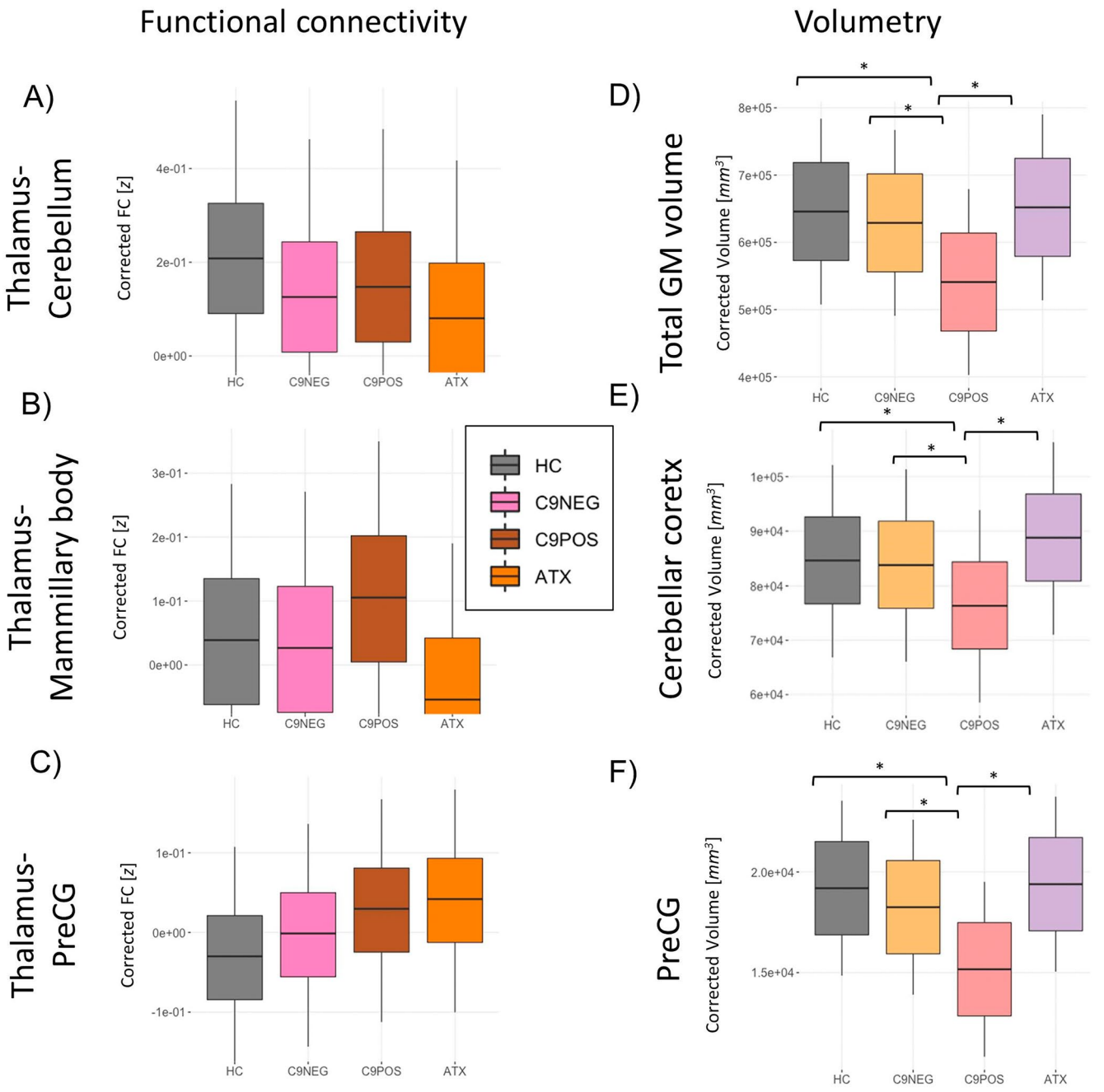

FIGURE 3 | Cross-sectional functional connectivity (FC) and volumetry. Baseline functional connectivity profiles are shown on the left (A-C) and baseline volume distributions on the right (D-F) * indicates adjusted *p*-values ≤ 0.05 in post-hoc pairwise comparisons using Tukey's HSD testing. Abbreviations: ATX, Patients with ALS carrying an intermediate length CAG repeat expansion in *ATXN2*; C9NEG, Sporadic patients with ALS testing negative for ALS associated genetic variants as well as *C9orf72* hexanucleotide repeat expansions; C9POS, Patients with ALS carrying GGGGCC hexanucleotide repeat expansions in *C9orf72*; HC, Healthy controls; PreCG, precentral gyrus.

can accurately map propagation patterns over time and help the development of sensitive monitoring markers with pragmatic utility in clinical trials [48]. Another factor to consider is that by the time patients fulfill diagnostic criteria and are recruited into research studies, some of their disease-defining brain regions (PreCG, CST) may already be very severely affected and further deterioration may be difficult to capture over time. This is sometimes referred to as ceiling or flooring effect. In our study, for example, we detect progressive motor cortex degeneration in the C9POS group, but not in the large sporadic C9NEG cohort. To comprehensively assess progressive changes, map spread patterns accurately and verify academic concepts such as 'prion-like propagation' etc., the recruitment of presymptomatic mutation carriers is probably the best approach, followed by their follow-up over many time points until phenoconversion and beyond. The few existing presymptomatic studies in ALS [49] consistently capture thalamic changes [31, 50, 51] sometimes before cortical changes are detectable [31]. These observations may suggest that subcortical and thalamic pathology are crucial seeds of disease spreads, but need to be verified in large prospective studies. It is also noteworthy that the descriptive statistics of academic

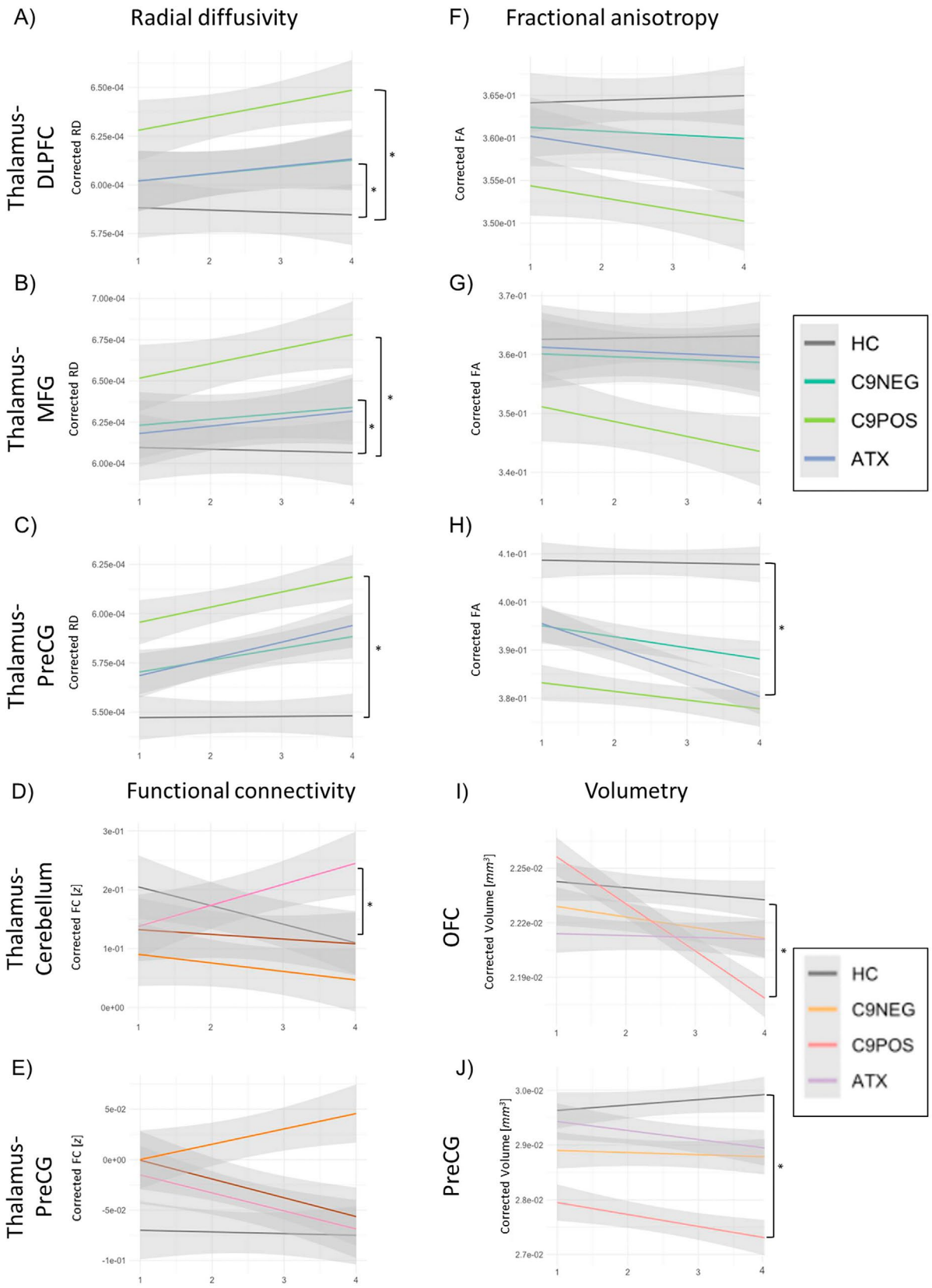

FIGURE 4 | Longitudinal findings. Progressive radial diffusivity (A-C) , fractional anisotropy (F-H), functional connectivity (D,E) and volumetric alterations (I,J) in the four study groups. * indicates *p*-values ≤ 0.05, comparing the interaction effect *Genotype X Time* versus *HC x Time* in a linear mixed effects model. Abbreviations: ATX, Patients with ALS carrying an intermediate length CAG repeat expansion in *ATXN2*; C9NEG, Sporadic patients with ALS testing negative for ALS associated genetic variants as well as *C9orf72* hexanucleotide repeat expansions; C9POS, Patients with ALS carrying GGGGCC hexanucleotide repeat expansions in *C9orf72*; DLPFC, dorsolateral prefrontal cortex; HC, Healthy controls; MFG, medial frontal gyrus, OFC, orbitofrontal cortex; PreCG, precentral gyrus.

TABLE 2 | Longitudinal trajectories in ALS genotypes versus healthy controls.

	Linear mixed effects models (comparing interaction effects: "Time × ALS Genotype" vs. "Time × HC")			
	Significant contrasts	***t*(DOF), *p***	**Significant contrasts**	***t*(DOF), *p***
Connectivity				
Connectivity: *Thalamus-Anterior cingulate cortex*			*Connectivity*: *Thalamus-Cerebellar cortex*	
SC:FA	—	—	—	—
SC:RD	—	—	—	—
FC	—	—	- Time × C9NEG—Time × HC	- $t(187) = 2.08$, $p = 0.039$
Connectivity: *Thalamus-Dorsolateral prefrontal cortex*			*Connectivity*: *Thalamus-Heschl's gyrus*	
SC:FA	—	—	—	—
SC: RD	- Time × C9NEG—Time × HC—Time × C9POS—Time × HC	- $t(194) = 2.18$, $p = 0.031$—$t(194) = 1.92$, $p = 0.056$	—	—
FC	- Time × ATX—Time × HC	- $t(187) = 2.10$, $p = 0.037$	—	—
Connectivity: *Thalamus-Mammillary bodies*			*Connectivity*: *Thalamus-Medial frontal gyrus*	
SC: FA	—	—	—	—
SC: RD	—	—	- Time × C9NEG—Time × HC—Time × C9POS—Time × HC	- $t(194) = 2.15$, $p = 0.033$—$t(194) = 2.38$, $p = 0.018$
FC	—	—	—	—
Connectivity: *Thalamus-Orbitofrontal cortex*			*Connectivity*: *Thalamus-Parietal cortex (no postcentral gyrus)*	
SC: FA	—	—	—	—
SC: RD	—	—	—	—
FC	—	—	—	—
Connectivity: *Thalamus-Postcentral gyrus*			*Connectivity*: *Thalamus-Precentral gyrus*	
SC: FA	—	—	- Time × ATX—Time × HC	- $t(194) = -2.05$, $p = 0.042$
SC: RD	- Time × C9NEG—Time × HC - Time × ATX—Time × HC	- $t(194) = 2.85$, $p = 0.005$—$t(194) = 2.41$, $p = 0.017$	- Time × C9NEG—Time × HC	- $t(194) = 2.44$, $p = 0.016$
FC	—	—	—	—
Connectivity: *Thalamus-V1*				
SC: FA	—	—		

(Continues)

TABLE 2 | (Continued)

	Linear mixed effects models (comparing interaction effects: "Time × ALS Genotype" vs. "Time × HC")			
	Significant contrasts	***t*(DOF), *p***	**Significant contrasts**	***t*(DOF), *p***
SC: RD	—	—		
FC	—	—		
Volumetry				
Volume: *Total grey matter volume*			*Volume*: *Thalamus*	
	- Time × ATX—Time × HC	- $t(200) = -1.92$, $p = 0.056$	—	—
Volume: *Anterior cingulate cortex*			*Volume*: *Cerebellar cortex*	
	—	—	- Time × C9NEG – Time × HC	- $t(200) = 2.08$, $p = 0.039$
Volume: *Dorsolateral prefrontal cortex*			*Volume*: *Heschl's gyrus*	
	—	—	—	—
Volume: *Mammillary bodies*			*Volume*: *Medial frontal gyrus*	
	—	—	—	—
Volume: *Orbitofrontal cortex*			*Volume*: *Parietal cortex* (*no postcentral gyrus*)	
	- Time × C9POS—Time × HC	- $t(200) = -3.00$, $p = 0.003$	—	—
Volume: Postcentral gyrus			*Volume*: *Precentral gyrus*	
	—	—	- Time × C9POS – Time × HC	- $t(200) = -2.17$, $p = 0.031$
Volume: *Primary visual cortex*				
	—	—		

Note: —, no significant contrasts for the tested effect in the linear mixed effects model.

Abbreviations: ALS, amyotrophic lateral sclerosis; ANOVA, analysis of variance; ATX, Patients with ALS carrying an intermediate length CAG repeat expansion in *ATXN2*; C9NEG, Sporadic patients with ALS testing negative for ALS-associated genetic variants as well as *C9orf72* hexanucleotide repeat expansions; C9POS, Patients with ALS carrying GGGGCC hexanucleotide repeat expansions in *C9orf72*; dMRI, diffusion-weighted magnetic resonance imaging; DOF, degrees of freedom; FA, fractional anisotropy; FC, functional connectivity; HC, healthy control; *n.a*, not applicable; RD, radial diffusivity; rs-fMRI, resting-state functional magnetic resonance imaging; SC, structural connectivity; T1w, T1-weighted.

imaging studies merely represent typical disease trajectories of a representative patient with a specific genotype and do not describe disease burden in an individual patient. There is a significant shift from group-level descriptive studies to characterize disease burden in individual patients [52, 53]. Tractography performed in 'subject-space' and cortical volume estimations in specific ROIs is an important step in the direction of assessing anatomical integrity in individual patients and potentially permits the tracking of pathology in a single, specific patient over time. The two important trends of neuroimaging in ALS are the evaluation of presymptomatic or incipient disease and the development of robust methods to describe disease burden patterns in single individuals. The former is important for phenoconversion predictions and the understanding of disease spread processes before the disease manifests and irreversible and widespread network changes have taken place [51]. The latter is important for the accurate and early categorization of patients into relevant diagnostic, phenotypic and prognostic categories. A number of machine-learning (ML) approaches have been developed and trialed in ALS to address these challenges [54], and significant developments are likely to be witnessed in the near future as larger and larger data sets are generated by various consortia.

This study is not without limitations. We have focused on the quantitative radiological evaluation of thalamic, thalamocortical and cortical changes in genetically screened patients with ALS and have intentionally not explored clinicoradiological correlations. Extra-motor deficits in ALS already have a considerable literature [55] and in this study we have specifically sought to describe thalamocortical dissociation in ALS genotypes without speculating on direct clinical correlates [56]. We also need to specifically acknowledge the small sample size of our ATX cohort. Moreover, the ALS cohort of this study had fewer years of education and relatively more males compared to controls. While we carefully correct for the effects of age, sex, handedness, and education in all of our statistical models, the literature on sexual dimorphism and education suggests that, ideally, study groups should be matched for all of these factors [57, 58]. We explored connectivity between well-defined anatomical regions, but other studies in ALS sometimes evaluate the connectivity of one specific region to the entire brain [59, 60]. Notwithstanding these limitations, our data demonstrate that thalamus-mediated circuits and cortico-thalamic and thalamo-cortical white matter projections succumb to progressive neurodegeneration. Our data add to the increasing consensus that ALS is a 'network disease' and its main clinical manifestations stem from gradual cortico-cortico, cortico-basal, cortico-cerebellar and cortico-spinal disconnection.

5 | Conclusions

The core symptoms of ALS are unlikely to stem from focal cortical or subcortical degeneration, but are rather the results of networkwise degeneration of susceptible circuits. The thalamus gets progressively isolated from its cortical connections in ALS due to gradual white matter degeneration. Thalamocortical white matter degeneration in ALS likely contributes to a multitude of cognitive, behavioral, somatosensory and extrapyramidal manifestations.

Author Contributions

Marlene Tahedl: conceptualization, investigation, writing – original draft, methodology, formal analysis. **Jana Kleinerova:** conceptualization, investigation, writing – original draft, methodology, formal analysis. **Mark A. Doherty:** investigation, formal analysis. **Jennifer C. Hengeveld:** investigation, formal analysis. **Russell L. McLaughlin:** investigation, formal analysis. **Orla Hardiman:** investigation, conceptualization. **Ee Ling Tan:** conceptualization, investigation, formal analysis, writing – original draft. **Peter Bede:** conceptualization, investigation, funding acquisition, writing – original draft, formal analysis, methodology.

Acknowledgements

We are most grateful for the participation of each patient and healthy control. We also thank all patients who expressed interest in this research study but were unable to participate due to medical or logistical reasons. We also express our gratitude to the caregivers and families of each patient for facilitating attendance at our research centre. Without their generosity, this study would not have been possible.

Ethics Statement

This study was approved by the Ethics (Medical Research) Committee—Beaumont Hospital, Dublin, Ireland (IRB).

Consent

All participants provided informed consent.

Conflicts of Interest

The authors declare no conflicts of interest.

Data Availability Statement

Due to departmental policies, clinical, demographic and imaging data from individual patients cannot be made publicly available. Further information on data processing can be requested from the corresponding author.

References

1. H. J. Westeneng, E. Verstraete, R. Walhout, et al., "Subcortical Structures in Amyotrophic Lateral Sclerosis," *Neurobiology of Aging* 36 (2015): 1075–1082.

2. P. Bede, T. Omer, E. Finegan, et al., "Connectivity-Based Characterisation of Subcortical Grey Matter Pathology in Frontotemporal Dementia and ALS: A Multimodal Neuroimaging Study," *Brain Imaging and Behavior* 12 (2018): 1696–1707.

3. M. Bocchetta, E. G. Todd, N. Y. Tse, et al., "Thalamic and Cerebellar Regional Involvement Across the ALS-FTD Spectrum and the Effect of C9orf72," *Brain Sciences* 12, no. 3 (2022): 336, https://doi.org/10.3390/brainsci12030336.

4. A. Cistaro, M. Pagani, A. Montuschi, et al., "The Metabolic Signature of C9ORF72-Related ALS: FDG PET Comparison With Nonmutated Patients," *European Journal of Nuclear Medicine and Molecular Imaging* 41 (2014): 844–852.

5. K. R. Sharma, G. Saigal, A. A. Maudsley, and V. Govind, "1H MRS of Basal Ganglia and Thalamus in Amyotrophic Lateral Sclerosis," *NMR in Biomedicine* 24 (2011): 1270–1276.

6. D. Lule, V. Diekmann, H. P. Muller, J. Kassubek, A. C. Ludolph, and N. Birbaumer, "Neuroimaging of Multimodal Sensory Stimulation in Amyotrophic Lateral Sclerosis," *Journal of Neurology, Neurosurgery, and Psychiatry* 81 (2010): 899–906.

7. M. Neumann, D. M. Sampathu, L. K. Kwong, et al., "Ubiquitinated TDP-43 in Frontotemporal Lobar Degeneration and Amyotrophic Lateral Sclerosis," *Science* 314 (2006): 130–133.

8. J. Brettschneider, K. Del Tredici, D. J. Irwin, et al., "Sequential Distribution of pTDP-43 Pathology in Behavioral Variant Frontotemporal Dementia (bvFTD)," *Acta Neuropathologica* 127 (2014): 423–439.

9. P. Bede, M. Elamin, S. Byrne, et al., "Basal Ganglia Involvement in Amyotrophic Lateral Sclerosis," *Neurology* 81 (2013): 2107–2115.

10. M. Bocchetta, J. E. Iglesias, M. Neason, D. M. Cash, J. D. Warren, and J. D. Rohrer, "Thalamic Nuclei in Frontotemporal Dementia: Mediodorsal Nucleus Involvement Is Universal but Pulvinar Atrophy Is Unique to C9orf72," *Human Brain Mapping* 41 (2020): 1006–1016.

11. J. D. Schmahmann, "Vascular Syndromes of the Thalamus," *Stroke* 34 (2003): 2264–2278.

12. R. P. Vertes, S. B. Linley, and W. B. Hoover, "Limbic Circuitry of the Midline Thalamus," *Neuroscience and Biobehavioral Reviews* 54 (2015): 89–107.

13. R. H. Tan, S. Wong, J. J. Kril, et al., "Beyond the Temporal Pole: Limbic Memory Circuit in the Semantic Variant of Primary Progressive Aphasia," *Brain* 137 (2014): 2065–2076.

14. F. Christidi, J. Kleinerova, E. L. Tan, et al., "Limbic Network and Papez Circuit Involvement in ALS: Imaging and Clinical Profiles in GGGGCC Hexanucleotide Carriers in C9orf72 and C9orf72-Negative Patients," *Biology (Basel)* 13 (2024): 504, https://doi.org/10.3390/biology13070504.

15. A. P. A. Bueno, L. C. de Souza, W. H. L. Pinaya, et al., "Papez Circuit Gray Matter and Episodic Memory in Amyotrophic Lateral Sclerosis and Behavioural Variant Frontotemporal Dementia," *Brain Imaging and Behavior* 15 (2021): 996–1006.

16. F. Trojsi, F. Di Nardo, G. Caiazzo, et al., "Hippocampal Connectivity in Amyotrophic Lateral Sclerosis (ALS): More Than Papez Circuit Impairment," *Brain Imaging and Behavior* 15 (2020): 2126–2138.

17. V. J. Kumar, E. van Oort, K. Scheffler, C. F. Beckmann, and W. Grodd, "Functional Anatomy of the Human Thalamus at Rest," *NeuroImage* 147 (2017): 678–691.

18. R. M. Bonelli and J. L. Cummings, "Frontal-Subcortical Circuitry and Behavior," *Dialogues in Clinical Neuroscience* 9 (2007): 141–151.

19. M. C. McKenna, P. Corcia, P. Couratier, W. F. Siah, P. F. Pradat, and P. Bede, "Frontotemporal Pathology in Motor Neuron Disease Phenotypes: Insights From Neuroimaging," *Frontiers in Neurology* 12 (2021): 723450, https://doi.org/10.3389/fneur.2021.723450.

20. M. C. McKenna, S. Li Hi Shing, A. Murad, et al., "Focal Thalamus Pathology in Frontotemporal Dementia: Phenotype-Associated Thalamic Profiles," *Journal of the Neurological Sciences* 436 (2022): 120221, https://doi.org/10.1016/j.jns.2022.120221.

21. M. C. McKenna, J. Lope, P. Bede, and E. L. Tan, "Thalamic Pathology in Frontotemporal Dementia: Predilection for Specific Nuclei, Phenotype-Specific Signatures, Clinical Correlates, and Practical Relevance," *Brain and Behavior: A Cognitive Neuroscience Perspective* 13, no. 2 (2023): e2881, https://doi.org/10.1002/brb3.2881.

22. C. O'Callaghan, M. Bertoux, and M. Hornberger, "Beyond and Below the Cortex: The Contribution of Striatal Dysfunction to Cognition and Behaviour in Neurodegeneration," *Journal of Neurology, Neurosurgery, and Psychiatry* 85, no. 4 (2013): 371–378, https://doi.org/10.1136/jnnp-2012-304558.

23. T. H. Bak and S. Chandran, "What Wires Together Dies Together: Verbs, Actions and Neurodegeneration in Motor Neuron Disease," *Cortex* 48 (2012): 936–944.

24. M. Grossman, C. Anderson, A. Khan, B. Avants, L. Elman, and L. McCluskey, "Impaired Action Knowledge in Amyotrophic Lateral Sclerosis," *Neurology* 71 (2008): 1396–1401.

25. T. Nonaka, M. Masuda-Suzukake, T. Arai, et al., "Prion-Like Properties of Pathological TDP-43 Aggregates From Diseased Brains," *Cell Reports* 4 (2013): 124–134.

26. J. D. Rohrer, J. M. Nicholas, D. M. Cash, et al., "Presymptomatic Cognitive and Neuroanatomical Changes in Genetic Frontotemporal Dementia in the Genetic Frontotemporal Dementia Initiative (GENFI) Study: A Cross-Sectional Analysis," *Lancet Neurology* 14 (2015): 253–262.

27. S. E. Lee, A. C. Sias, M. L. Mandelli, et al., "Network Degeneration and Dysfunction in Presymptomatic C9ORF72 Expansion Carriers," *NeuroImage Clinical* 14 (2016): 286–297.

28. A. Bertrand, J. Wen, D. Rinaldi, et al., "Early Cognitive, Structural, and Microstructural Changes in Presymptomatic C9orf72 Carriers Younger Than 40 Years," *JAMA Neurology* 75 (2018): 236–245.

29. M. Bocchetta, E. G. Todd, G. Peakman, et al., "Differential Early Subcortical Involvement in Genetic FTD Within the GENFI Cohort," *NeuroImage: Clinical* 30 (2021): 102646.

30. C. Cury, S. Durrleman, D. M. Cash, et al., "Spatiotemporal Analysis for Detection of Pre-Symptomatic Shape Changes in Neurodegenerative Diseases: Initial Application to the GENFI Cohort," *NeuroImage* 188 (2019): 282–290.

31. P. Bede, D. Lulé, H. P. Müller, et al., "Presymptomatic Grey Matter Alterations in ALS Kindreds: A Computational Neuroimaging Study of Asymptomatic C9orf72 and SOD1 Mutation Carriers," *Journal of Neurology* 270 (2023): 4235–4247.

32. C. J. Mahoney, L. E. Downey, G. R. Ridgway, et al., "Longitudinal Neuroimaging and Neuropsychological Profiles of Frontotemporal Dementia With C9ORF72 Expansions," *Alzheimer's Research & Therapy* 4, no. 5 (2012): 41, https://doi.org/10.1186/alzrt144.

33. M. Tahedl, E. L. Tan, R. H. Chipika, et al., "Brainstem-Cortex Disconnection in Amyotrophic Lateral Sclerosis: Bulbar Impairment, Genotype Associations, Asymptomatic Changes and Biomarker Opportunities," *Journal of Neurology* 270 (2023): 3511–3526.

34. G. E. Alexander, M. R. DeLong, and P. L. Strick, "Parallel Organization of Functionally Segregated Circuits Linking Basal Ganglia and Cortex," *Annual Review of Neuroscience* 9 (1986): 357–381, https://doi.org/10.1146/annurev.ne.09.030186.002041.

35. P. Bede, R. H. Chipika, F. Christidi, et al., "Genotype-Associated Cerebellar Profiles in ALS: Focal Cerebellar Pathology and Cerebro-Cerebellar Connectivity Alterations," *Journal of Neurology, Neurosurgery, and Psychiatry* 92 (2021): 1197–1205.

36. M. Tahedl, E. L. Tan, J. Kleinerova, et al., "Progressive Cerebrocerebellar Uncoupling in Sporadic and Genetic Forms of Amyotrophic Lateral Sclerosis," *Neurology* 103 (2024): e209623.

37. M. F. Rushworth, T. E. Behrens, and H. Johansen-Berg, "Connection Patterns Distinguish 3 Regions of Human Parietal Cortex," *Cerebral Cortex* 16, no. 10 (2006): 1418–1430, https://doi.org/10.1093/cercor/bhj079.

38. M. Abidi, P. F. Pradat, N. Termoz, A. Couillandre, P. Bede, and G. de Marco, "Motor Imagery in Amyotrophic Lateral Sclerosis: An fMRI Study of Postural Control," *NeuroImage. Clinical* 35 (2022): 103051.

39. M. Feron, A. Couillandre, E. Mseddi, et al., "Extrapyramidal Deficits in ALS: A Combined Biomechanical and Neuroimaging Study," *Journal of Neurology* 265 (2018): 2125–2136.

40. T. Burke, M. Elamin, P. Bede, et al., "Discordant Performance on the Reading the Mind in the Eyes Test, Based on Disease Onset in Amyotrophic Lateral Sclerosis," *Amyotrophic Lateral Sclerosis & Frontotemporal Degeneration* 17 (2016): 467–472.

41. M. Abidi, G. de Marco, F. Grami, et al., "Neural Correlates of Motor Imagery of Gait in Amyotrophic Lateral Sclerosis," *Journal of Magnetic Resonance Imaging* 53 (2021): 223–233.

42. H. Barbas, M. García-Cabezas, and B. Zikopoulos, "Frontal-Thalamic Circuits Associated With Language," *Brain and Language* 126 (2013): 49–61.

43. W. Yang, S. L. Tipparaju, G. Chen, and N. Li, "Thalamus-Driven Functional Populations in Frontal Cortex Support Decision-Making," *Nature Neuroscience* 25 (2022): 1339–1352.

44. Y. Wang, "Thalamus and Its Functional Connections With Cortical Regions Contribute to Complexity-Dependent Cognitive Reasoning," *Neuroscience* 562 (2024): 125–134.

45. P. Bede, U. Bogdahn, J. Lope, K. M. Chang, S. Xirou, and F. Christidi, "Degenerative and Regenerative Processes in Amyotrophic Lateral Sclerosis: Motor Reserve, Adaptation and Putative Compensatory Changes," *Neural Regeneration Research* 16 (2021): 1208–1209.

46. M. Abidi, G. de Marco, A. Couillandre, et al., "Adaptive Functional Reorganization in Amyotrophic Lateral Sclerosis: Coexisting Degenerative and Compensatory Changes," *European Journal of Neurology* 27 (2020): 121–128.

47. J. Kleinerova, M. Tahedl, E. L. Tan, et al., "Supra- and Infratentorial Degeneration Patterns in Primary Lateral Sclerosis: A Multimodal Longitudinal Neuroradiology Study," *Journal of Neurology* 271 (2024): 3239–3255.

48. R. H. Chipika, E. Finegan, S. Li Hi Shing, O. Hardiman, and P. Bede, "Tracking a Fast-Moving Disease: Longitudinal Markers, Monitoring, and Clinical Trial Endpoints in ALS," *Frontiers in Neurology* 10 (2019): 229, https://doi.org/10.3389/fneur.2019.00229.

49. R. H. Chipika, W. F. Siah, M. C. McKenna, S. Li Hi Shing, O. Hardiman, and P. Bede, "The Presymptomatic Phase of Amyotrophic Lateral Sclerosis: Are We Merely Scratching the Surface?," *Journal of Neurology* 268 (2021): 4607–4629.

50. J. Wen, H. Zhang, D. C. Alexander, et al., "Neurite Density Is Reduced in the Presymptomatic Phase of C9orf72 Disease," *Journal of Neurology, Neurosurgery, and Psychiatry* 90 (2019): 387–394.

51. K. van Veenhuijzen, H. H. G. Tan, A. D. Nitert, et al., "Longitudinal Magnetic Resonance Imaging in Asymptomatic C9orf72 Mutation Carriers Distinguishes Phenoconverters to Amyotrophic Lateral Sclerosis or Amyotrophic Lateral Sclerosis With Frontotemporal Dementia," *Annals of Neurology* 97 (2025): 281–295.

52. M. Tahedl, S. Li Hi Shing, E. Finegan, et al., "Propagation Patterns in Motor Neuron Diseases: Individual and Phenotype-Associated Disease-Burden Trajectories Across the UMN-LMN Spectrum of MNDs," *Neurobiology of Aging* 109 (2021): 78–87.

53. M. Tahedl, R. H. Chipika, J. Lope, S. Li Hi Shing, O. Hardiman, and P. Bede, "Cortical Progression Patterns in Individual ALS Patients Across Multiple Timepoints: A Mosaic-Based Approach for Clinical Use," *Journal of Neurology* 268 (2021): 1913–1926.

54. P. Bede, A. Murad, J. Lope, et al., "Phenotypic Categorisation of Individual Subjects With Motor Neuron Disease Based on Radiological Disease Burden Patterns: A Machine-Learning Approach," *Journal of the Neurological Sciences* 432 (2021): 120079.

55. F. Christidi, E. Karavasilis, M. Rentzos, N. Kelekis, I. Evdokimidis, and P. Bede, "Clinical and Radiological Markers of Extra-Motor Deficits in Amyotrophic Lateral Sclerosis," *Frontiers in Neurology* 9, no. 1005 (2018): 1005, https://doi.org/10.3389/fneur.2018.01005.

56. E. Verstraete, M. R. Turner, J. Grosskreutz, M. Filippi, and M. Benatar, "Mind the Gap: The Mismatch Between Clinical and Imaging Metrics in ALS," *Amyotrophic Lateral Sclerosis & Frontotemporal Degeneration* 16, no. 7-8 (2015): 524–529, https://doi.org/10.3109/21678421.2015.1051989.

57. P. Bede, M. Elamin, S. Byrne, and O. Hardiman, "Sexual Dimorphism in ALS: Exploring Gender-Specific Neuroimaging Signatures," *Amyotrophic Lateral Sclerosis & Frontotemporal Degeneration* 15 (2014): 235–243.

58. A. Seyedsalehi, V. Warrier, R. A. I. Bethlehem, B. I. Perry, S. Burgess, and G. K. Murray, "Educational Attainment, Structural Brain Reserve and Alzheimer's Disease: A Mendelian Randomization Analysis," *Brain* 146 (2023): 2059–2074.

59. F. Trojsi, F. Di Nardo, G. D'Alvano, et al., "Resting State fMRI Analysis of Pseudobulbar Affect in Amyotrophic Lateral Sclerosis (ALS): Motor Dysfunction of Emotional Expression," *Brain Imaging and Behavior* 17, no. 1 (2023): 77–89, https://doi.org/10.1007/s11682-022-00744-4.

60. F. Trojsi, F. Di Nardo, G. Caiazzo, et al., "Hippocampal Connectivity in Amyotrophic Lateral Sclerosis (ALS): More Than Papez Circuit Impairment," *Brain Imaging and Behavior* 15 (2021): 2126–2138.

Supporting Information

Additional supporting information can be found online in the Supporting Information section.